Chen
Journal of Engineering and Applied Science (2023) 70:26
https://doi.org/10.1186/s44147-023-00197-6

Journal of Engineering and Applied Science

RESEARCH Open Access

Dynamic and loss analysis of flood inundation in the floodplain area of the lower Yellow River considering ecological impact

Jie Chen[1*]

*Correspondence:
hdchenjie_111@126.com

[1] Yellow River Conservancy Technical Institute, Kaifeng 475004, Henan, China

Abstract

The floodplain area in the lower Yellow River plays the function of flood detention and undertakes the production and living functions of residents. Because the Yellow River basin is one of the most serious flooding areas in China, the Yellow River seriously threatens the safety of people's lives and property and social stability and development in the floodplain area. It is significant to carry out flood inundation dynamic analysis and flood loss assessment in the lower Yellow River. Taking the zonal flood detention of the Jiahetan-Gaocun section as an example, a two-dimensional flow mathematical model is established by using MIKE 21. Through the numerical simulation of flood routing during the flood detention operation, the flood detention effect of the floodplain area is analysed, and the flood inundation dynamic analysis and flood inundation loss evaluation are carried out. The results show that the maximum absolute error of water level calculated by the model in the measuring station is only 0.77 m. So, it is reliable to use MIKE 21 to simulate the flood process and flood diversion in the lower Yellow River. The flood with a peak discharge of 4000 m^3/s and 7000 m^3/s basically reaches the maximum submerged area after 100 h, with the maximum submerged areas of 173.72 km^2 and 323.47 km^2, respectively. Autumn grain, as the main source of income for floodplain residents, is severely lost in shallow water depth, so they are severely lost in both floods. Therefore, when opening a floodplain as a flood storage and detention area, it is important to consider their loss. The flood simulation analysis results and flood inundation loss evaluation results can provide a scientific basis for the rational utilization of flood storage and detention areas in the lower Yellow River.

Keywords: Lower Yellow River, Floodplain area, Flood detention basin, Flood inundation loss, MIKE 21

Introduction

The Yellow River, the second largest river in China, with a total basin population accounting for more than 30% of China's total population and a regional GDP of about 26% of the country [1], can be said to be an important ecological defense and economic belt in China. The Yellow River is recognized as one of the most complex rivers in the world because of its less water, more sediment, and unbalanced relationship between water and sediment, and frequent flood disasters [2, 3]. As the intensity

of extreme precipitation events increases with global warming [4, 5], the number of flood-susceptible areas and the population affected by floods [6] will increase in the future. The Yellow River basin is facing the impact of floods caused by extreme precipitation events [7, 8].

As a flood storage and detention area, the Yellow River floodplain area is located between the main channel of the lower Yellow River and the river banks on both banks. It is not only the main flood discharge place for the Yellow River to divide the flood and sediment but also an important ecological space and production space in the Central Plains of China. Due to natural conditions and human activities, the floodplain area is facing the problems of a fragile ecological environment and a low level of regional development [9].

Numerous scholars have conducted studies on the management of the lower Yellow River floodplain area. Yu and Gong [10] took the planning and design of the Yellow River floodplain area in Zhengzhou as an example to provide a reference for the ecological restoration of the floodplain area. Liu et al. [11] studied different governance modes of the Yellow River floodplain area and concluded that the floodplain area above Gaocun should build a high-standard protective embankment, and the floodplain area below Gaocun should implement the inundation compensation policy. Run et al. [12] studied the temporal and spatial dynamic changes of water and soil in the floodplain area based on the Google Earth Engine platform, which provides a reference for the comprehensive management of the floodplain area. According to the historical data of the Yellow River, Su et al. [13] put forward the exploratory preliminary governance model of three floodplains in the floodplain area of the wide reach of the lower Yellow River.

The general idea of environmental management in the floodplain area of the lower Yellow River divides the dike to the main channel into three parts: high floodplain, second floodplain, and tender floodplain [14]. Different flood control standards are set in each region, and the areas that fail to meet the standard are transformed and managed. The flood process has seriously affected the ecological management process of the beach area in the lower Yellow River. The task of beach area ecological governance mainly includes the construction of flood control and security projects to stabilize the river channel and control the river regime and the ecological governance of silted floodplain areas.

By building water conservancy projects or using areas with impoundment functions, reducing flood peak flow and allowing floods to occur in certain areas within a certain period of time can effectively reduce damage and protect society and development [15, 16]. The flood storage and detention area [17, 18] on the lower Yellow River floodplain area are an important part of the flood control system. It plays a certain role in peak shaving and flood detention in flood control emergency, to reduce the flood control pressure of the lower reaches. It is an important means and effective measure for flood control regulation. The flood discharge capacity of the floodplain area can generally account for about 20% of the full section flow during large floods. However, due to human activities in the floodplain area, the flood storage and detention area should not only consider reducing the downstream flood risk but also consider reducing the economic loss in the process of flood diversion and detention in the flood storage and detention area [19]. Therefore, it is of great significance to the dynamic analysis and loss assessment of flood inundation in the floodplain area of the lower Yellow River.

Flood damage assessment [20, 21] is the process of analysing and quantifying the consequences caused by floods. Many scholars have used different methods to evaluate the loss of flood disasters in different areas and carry out flood risk management work. Chinh et al. [22] used multivariate statistical analysis to analyse the flood loss of residential buildings in Cantor city in the Mekong Delta. Zhao et al. [23] used the coupling of the SWMM and MIKE 21 model to analyse the flood inundation loss in the central area of Cangzhou, Hebei. Guo et al. [24] created a flood risk assessment model of flood storage and detention area based on a mechanical process to quantitatively evaluate the flood risk level of flood storage and detention area during the commissioning of flood diversion and storage project. Gemmer et al. [25] evaluated the dynamic loss of flood inundation in the Honghu flood diversion, storage, and detention area by using the two-dimensional hydrological hydrodynamic model based on GIS data. With the progress of artificial intelligence technology, more and more scholars use machine learning and optimization algorithm to analyse flood damage assessment. Ruidas et al. [26] build new GIS-based ensemble models based on Support Vector Regression and two meta-heuristic optimization algorithms for flash flood-susceptibility mapping. Ruidas et al. [27] propose to draw the flash flood hazard map using the bivariate logistic regression. Roy et al. [28] use the biogeography-based optimization model in GIS environment to present the flood sustainable areas. Schröter et al. [29] used a 3D urban model and random forest to analyse urban flood loss, inundation loss, and risk.

Based on flood process simulation, scholars have conducted extensive research on flood inundation loss assessment, and its main steps can be summarized as the following four steps.

1. According to the flood analysis model, calculate and determine the flood inundation range, water depth, duration, velocity, and other key indicators.
2. Obtain the value and distribution of different properties under different inundation depths and durations within the flood inundation range.
3. According to the analysis of survey data, establish the relationship between submerged water depth, duration, velocity, and other factors and flood inundation loss rate of various properties.
4. Calculate the property loss of flood disaster according to the relationship between various property types and the flood loss rate in the flooded area.

At present, the submerged depth-loss rate relationship method [30] is mostly used to study the relationship between the submerged loss rate of various properties and different floods, and its function forms are diverse. For example, James and Lee [31] were the first to give a segmented linear urban property inundation water depth-loss rate function. Zhang et al. [32] used the relationship function between inundation water depth and inundation loss for different disaster-bearing bodies to establish an inundation loss assessment system for flooding in the lower Yellow River floodplain area. In summary, we found that the accuracy of data such as inundation depth, inundation duration, and water velocity has a significant impact on the effectiveness of flood loss prediction. Therefore, to make a good flood loss prediction, we need to make a good flood simulation. Numerical simulation of flood evolution serves as the basis for flood

risk mapping, flood risk analysis, and flood damage assessment and is the scientific basis for flood management. In this paper, we propose to perform flood evolution simulation calculations using MIKE software, which is a powerful and easy-to-use model that has been widely used [33]. Liu et al. [34] established the one-dimensional MIKE 11 model, two-dimensional MIKE 21 model, and one- and two-dimensional dynamically coupled MIKE FLOOD model based on the principles and methods of the MIKE series. They verified that the flood simulation model constructed based on MIKE can better simulate the evolution of floods in the flood storage area through actual data. Based on the MIKE 21 model, Chen et al. [35] analysed the evolution process of 50-year return period flood under the current conditions of Daluze and Ningjinbo flood storage and detention area. Zhang and Li [36] established the model of the reach from Huayuankou to Jiahetan by using the MIKE 21 model, which proved the feasibility of MIKE 21 in simulating the hydraulic problems in the lower Yellow River floodplain area.

In order to better manage the floods in the lower Yellow River, explore the flood inundation law of the floodplain area of the lower Yellow River as a flood storage and detention area and determine the key points of flood inundation losses in the floodplain area of the lower Yellow River; in this study, the Jiahetan-Gaocun reach of the lower Yellow River will be selected as a typical reach, which includes the Dongming floodplain area and Changyuan floodplain area. Based on the MIKE 21 model, the flood routing process under two different working conditions will be simulated for the floodplain area of the reach, and the flood inundation dynamic process and flood inundation loss analysis will be analysed, to provide a reference for the planning and management of the floodplain area of the lower Yellow River.

Methods and model

MIKE 21

Compared with the data-driven model represented by machine learning [37–40], the hydrodynamic model can better simulate various situations we want. The MIKE 21 has a powerful function in the numerical simulation of planar two-dimensional free surface flow. It is suitable for simulating hydrodynamic and environmental phenomena in lakes, estuaries, bays, coasts, and oceans when the vertical velocity and acceleration can be ignored when the horizontal scale is much larger than the vertical scale. The MIKE 21 [41] hydrodynamic model is based on the Navier–Stokes equation of momentum conservation of two-dimensional viscous incompressible fluid and is subject to the Boussinesq and hydrostatic pressure assumptions. The two-dimensional shallow water equations are obtained by assuming a hydrostatic pressure distribution and integrating the Navier–Stokes equations over the water depth. Compared with empirical formula and physical model, this model is more accurate. The main governing equations of the MIKE 21 model [42] are as follows. And the governing equations are solved in a Cartesian coordinate system.

$$\frac{\partial h}{\partial t} + \frac{\partial hu}{\partial x} + \frac{\partial hv}{\partial y} = hS$$

Two-dimensional flow momentum equation is as follows:

$$\frac{\partial hu}{\partial t}+\frac{\partial hu^2}{\partial x}+\frac{\partial hvu}{\partial y}=fhv-gh\frac{\partial \eta}{\partial x}-\frac{h}{\rho}\frac{\partial p_A}{\partial x}-\frac{gh^2}{2\rho}\frac{\partial \rho}{\partial x}-\frac{\tau_{fx}}{\rho}+\frac{\tau_{sx}}{\rho}-F_{vx}+\frac{\partial hT_{xx}}{\partial x}+\frac{\partial hT_{xy}}{\partial y}+hu_sS$$

$$\frac{\partial hv}{\partial t}+\frac{\partial hv^2}{\partial x}+\frac{\partial hvu}{\partial x}=-fhu-gh\frac{\partial \eta}{\partial y}-\frac{h}{\rho}\frac{\partial p_A}{\partial y}-\frac{gh^2}{2\rho}\frac{\partial \rho}{\partial y}-\frac{\tau_{fy}}{\rho}+\frac{\tau_{sy}}{\rho}-F_{vy}++\frac{\partial hT_{xy}}{\partial x}+\frac{\partial hT_{yy}}{\partial y}+hv_sS$$

In the formula, t represents time. x and y are the Cartesian coordinates. u and v are the components of average velocity in x and y directions respectively. η represents water level. d is static water depth. h indicates total water depth, $h = d + \eta$. g is the acceleration of gravity. f is the Koch force coefficient. p_A is atmospheric pressure. τ_{sx}, τ_{sy}, τ_{fx}, and τ_{fy} are surface wind stress and bottom shear stress in x and y directions. ρ is the water density. T_{xx}, T_{xy}, and T_{yy} are the horizontal viscous stress term.u_s and v_s are the source term flow velocity. S is source term.

Model establishment

Model calculation range

Based on the research task of this flood simulation, the topographic characteristics of the river channel in the lower Yellow River, river flood characteristics, production dikes, and other influencing factors are also taken as the principles of model scope determination. The model range selected for this simulation is as follows: the upper boundary is Jiahetan, the lower boundary is the Gaocun, the total longitudinal length of the simulation range is about 73.5 km, and the simulated horizontal width is 5.5–20 km. This reach includes Dongming and Changyuan floodplain areas.

Gridding and terrain treatment

This simulation uses the MIKE 21 unstructured grid, and the model solution is solved by the finite volume method of the unstructured grid central grid. The calculation area uses an irregular triangular grid, and the main channel part needs to be encrypted, using a maximum grid area of 50,000 m^2 and a maximum grid area of 100,000 m^2 for the rest of the area. The results of the model simulation area grid profile are shown in Fig. 1.

Terrain processing is the key step in modeling. The quality of terrain processing is directly related to the accuracy of the model. The terrain processing in this calculation includes the main channel of the Jiahetan-Gaocun section and floodplain terrain processing.

In this simulation, the main channel of the Jiahetan-Gaocun section and floodplain terrain data is based on the Yellow River Water Resources Commission Design Institute mapping team in July 1998 to draw a ratio of 1:1,000,000 digital mapping by the digital instrument into Beijing coordinates and then converted to MIKE UTM coordinates. Then, the terrain data file of the river is imported into the grid for internal difference, and the final simulation area topographic map is shown in Fig. 2.

Boundary condition

Before establishing the MIKE 21 flow model, input data must be created according to measured data.

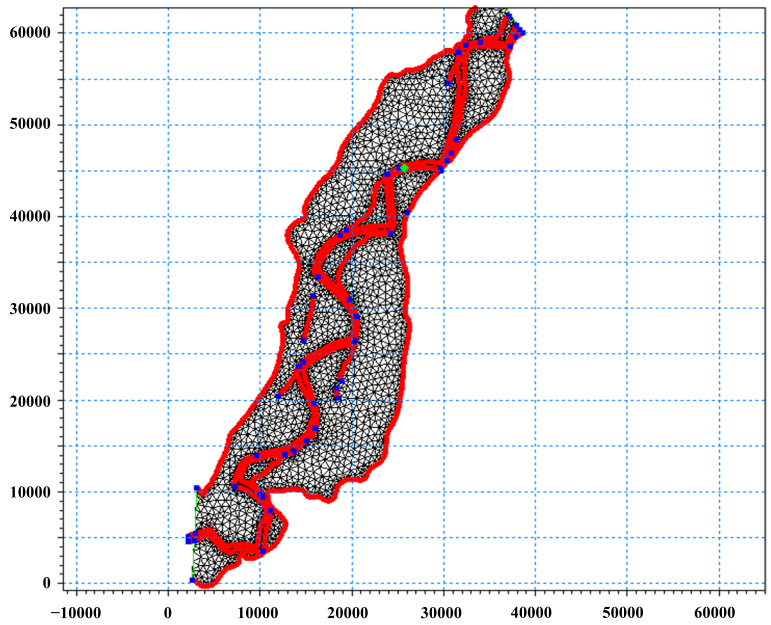

Fig. 1 Computational grid diagram

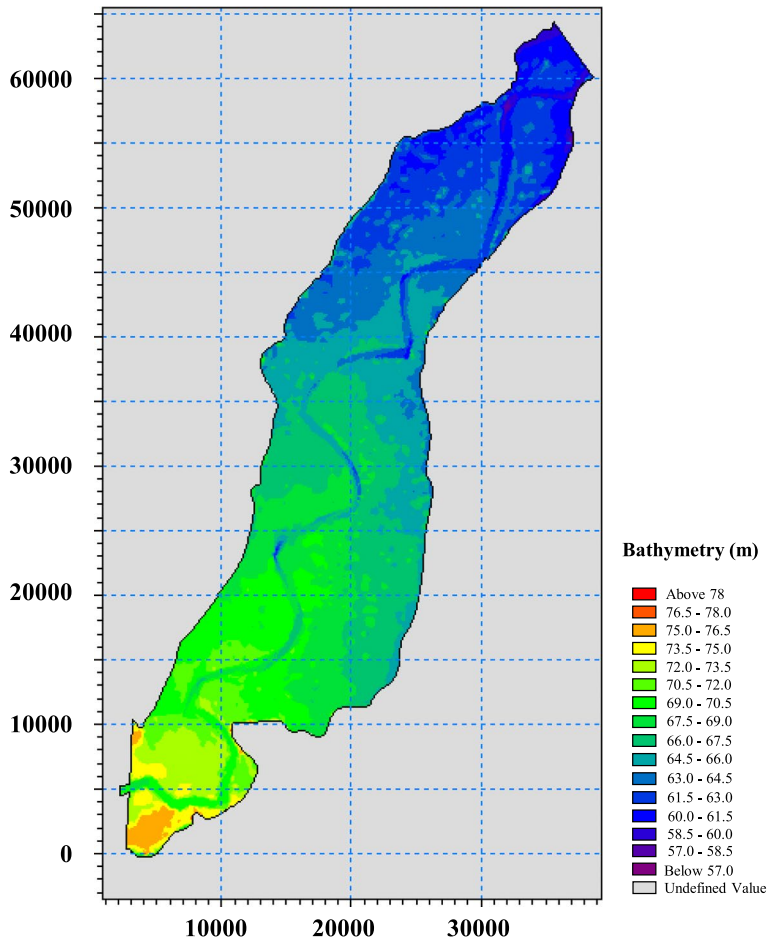

Fig. 2 Topographic map of the calculation area

In the input conditions of this study, the upstream import conditions adopt the flood flow process; the downstream outlet boundary condition uses the water level-time relationship as the control open boundary condition. According to the principle that the fluid wall cannot pass through, without considering the infiltration, the normal velocity on the land boundary can be considered to be 0. According to the principle of water flow without sliding, the tangential velocity of water on the land boundary should also be 0.

Initial condition

Before the simulation calculation, it is assumed that there is no water in the floodplain area, so the initial condition is set to the initial water level value, and the initial water level in the main channel part of this simulation is 0.5 m, and the water level in the floodplain is 0.

Dynamic boundary processing

For the calculation of the process of dry and wet floodplain in the region, the water level discrimination method [43, 44] is used to deal with, that is, when the water depth at a certain point is less than the dry water depth of 0.005 m, so that the flow velocity at the place is zero, the floodplain dries out and does not participate in the calculation; when the water depth at the place is greater than the wet water depth of 0.1 m, the floodwater on the floodplain participates in the calculation.

Model simulation validation and parameter adjustment

To ensure that the 2D mathematical model can correctly simulate the flood evolution in the calculation area, this flood simulation needs to rate the Manning coefficient (n), which mainly reflects the roughness of the riverbed.

The model rate was set using the measured water level of the August 1996 flood. The "96.8" flood was medium, and the floodwater had already spread out of the channel, which could reflect to a certain extent the flooding condition of the channel and the resistance condition of the channel. In the inversion of the historical flood, the flood process is adopted before and after the flood peak of "96.8" (the starting flow is around 1500 m^3/s, and the ending flow is around 2000 m^3/s), totaling 408 h.

In the process of model rate determination, different roughness of floodplain and trough were used to simulate the flow resistance, and the roughness of river trough was generally taken as $n = 0.011 \sim 0.015$, and the roughness of floodplain was taken as $n = 0.02 \sim 0.03$. Under such boundary conditions, the model was commissioned to invert the "96.8" flood in the calculation area. In the process of debugging, we considered the characteristics of narrow river channel in the lower Yellow River, large zigzag rate in the local river section, and serious erosion of the channel side during the "96.8" flood and selected a larger moving bed roughness $n = 0.014 \sim 0.017$. The influence of channel morphology on overflow is reflected more realistically, and it is convenient to calibrate the flood level more reasonably. From the comparison results in Table 1, it can be seen that the calculated water level at the flood level observation point and the measured water level basically match, and the mathematical model used in this simulation is basically

Table 1 Comparison of measured water level and simulated water level

No	Name of measuring station	Measured value (m)	Simulated value (m)	Error (m)
1	Dongbatou	73.4800	73.6808	0.2008
2	Chanfang	72.8400	72.6977	−0.1423
3	Shitouzhuang	67.8200	67.5323	−0.2877
4	Yulin	65.9700	66.1667	0.1967
5	Qingzhuang	63.2000	63.9728	0.7728

correct in the selection of control parameters such as river topography treatment and roughness selection, and the constructed planar 2D mathematical model can correctly simulate the flood evolution in the calculation area.

Results and discussion

Calculation scheme and condition setting

The simulation is designed for the characteristics of floods in the lower Yellow River, and the simulated floods are divided into two levels: the first level flood with a peak flow of about 4000 m^3/s, which is close to the flood of flat floodplain, and the "92.8" flood process is chosen as a typical flood; the second level flood with a peak flow of about 7000 m^3/s, which is a medium flood, and the "96.8" flood process is chosen as a typical flood. The flood processes of "92.8" and "96.8" are shown in Figs. 3 and 4.

According to the two typical flood conditions, the numerical simulation of nonconstant flow is carried out in accordance with the boundary conditions of the planned control zone flood control (construction of planned flood control levees, with the standard that the flood does not spread the levees).

The calculation conditions are based on the simulation of flood propagation in two frequency floods of the river under the stagnant boundary conditions of the planning control zone, and there are two combinations; see Table 2. Both combinations are abolished for the dangerous control treatment, the production dike treatment, and the village treatment. By numerical simulation of the planar 2D water flow in the river section under the boundary conditions of the stagnant work condition and also setting up the

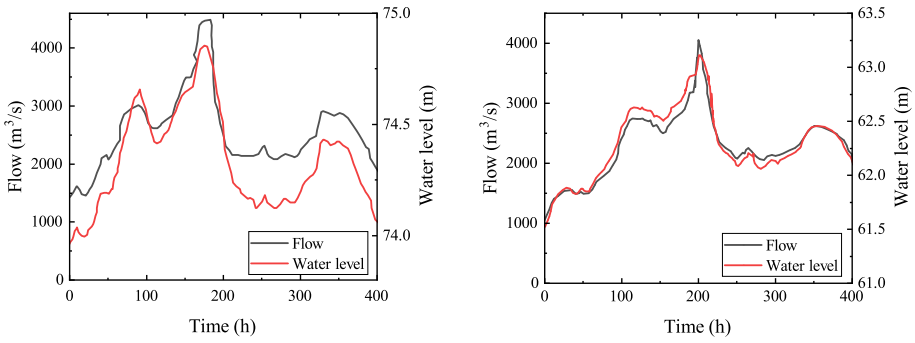

Fig. 3 "92.8" flood process. **a** Jiahetan. **b** Gaocun

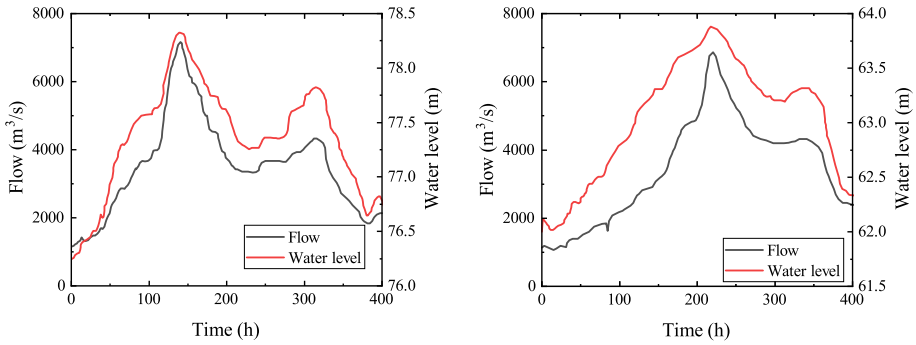

Fig. 4 "96.8" flood process. **a** Jiahetan. **b** Gaocun

Table 2 Calculation conditions and boundary conditions

Flood type	Boundary condition	Floodplain area treatment
"92.8"	Flood detention condition	Build a flood detention dike to ensure that the flood does not overflow the dike. Dongming floodplain area stagnant use
"96.8"	Flood detention condition	Build a flood detention dike to ensure that the flood does not overflow the dike. Changyuan floodplain area and Dongming floodplain area stagnant use

controlled flood separation application in different stagnant zones of the floodplain area, the data on the evolutionary changes of the river flood, the inundation range at different time periods, and different water depths are obtained.

Calculation results

The inundation areas of different water depths at different time periods under two different flood conditions are shown in Figs. 5 and 6 below, which is composed of the areas of different water depths and corresponding water depths within the floodplain inundation area. The inundation water level is an important factor affecting the enclosure and safety zone, and the inundation water depth is the basic information for estimating the inundation loss. This design takes the inundation water depth can be divided into < 0.5-m shallow water, 0.5–2-m medium water, 2–4-m deep water, and > 4 m very deep water, a total of four levels. The time course of the inundation area under two different flood conditions is shown in Figs. 7 and 8 below. The numerical simulation results at different times are shown in Figs. 9 and 10.

Analysis of calculation results

From the simulation results of the typical floods of "92.8" and "96.8" above, we can see the following:

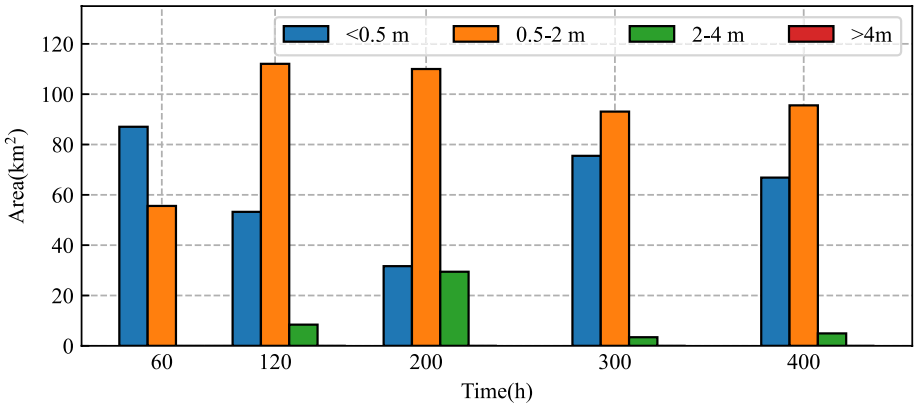

Fig. 5 Water depth and inundation area in different periods of "92.8" flood

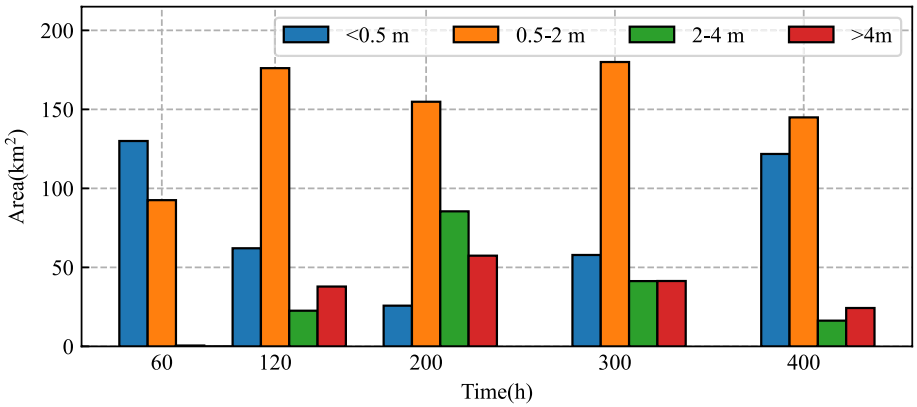

Fig. 6 Water depth and inundation area in different periods of "96.8" flood

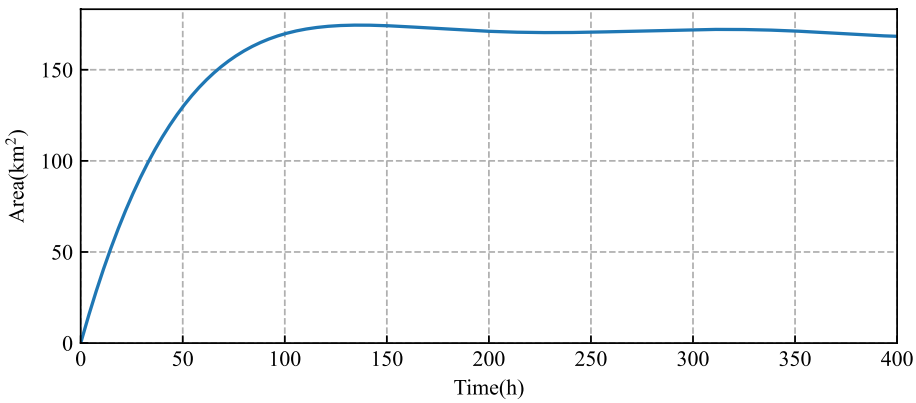

Fig. 7 "92.8" flood inundation area time history

1. As the flooding process advances, the inundation area of the floodplain gradually increases, and the flood loss in the floodplain also gradually increases. After a certain time, the inundation area stabilizes, and the loss reaches the maximum. The inundation area of "92.8" flood reaches the maximum at 120 h of operation, and the inunda-

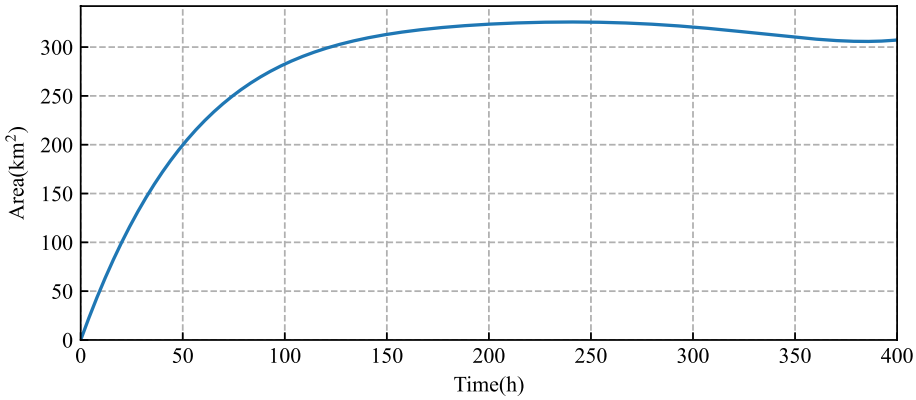

Fig. 8 "96.8" flood inundation area time history

tion area is 173.72 km^2. The inundation area of "96.8" flood reaches the maximum at 180 h of operation, and the inundation area is 323.47 km^2.

2. The inundation area of different water depths changes with time and flow rate. In the pre-flood period with a small flow rate, the shallow water depth area and medium water depth inundation area accounted for most of the area due to the speed of flood evolution. With the increase of flow and time, the shallow deepwater area and medium-deep water inundation area gradually decrease, and the deepwater area and very deep water area gradually increase to a certain time tends to the maximum, at which time the inundation loss of the stagnant area is the maximum. With the passing of the flood peak, the area of deep water and very deep water gradually decreases and returns to the situation where shallow water area and medium water area are dominant.
3. The flood flow of "96.8" is larger than that of "92.8," and in the simulation, the flood conditions of "96.8" open the Dongming floodplain area and the Changyuan floodplain area. Therefore, the maximum inundation area of the "96.8" flood detention area is 323.47km^2, while the maximum inundation area of the "92.8" flood detention area is 323.47 km^2. Therefore, the maximum inundation area of "96.8" flood stagnation zone is 323.47km^2, and the maximum inundation area of "92.8" flood stagnation zone is 173.72 km^2; the inundation area of "96.8" flood is 86.2% larger than that of "92.8" flood, and the inundation loss is also larger accordingly. In the "92.8" flood, there was no very deep water with a depth greater than 4 m.

The floods of "92.8" and "96.8" of different magnitudes basically reached the maximum inundation area after 100 h. The flood of "92.8" only used the Dongming floodplain area, while the flood of "96.8" used the Dongming and Chang Yuan floodplain areas. The flood of "96.8" inundated 149.75 km^2 more than the flood of "92.8." Chen et al. [45] also used the "96.8" flood to study the impact of opening this two floodplains on river flood control, with a total submerged area of 339.5 km^2. Wang et al. [46] have used numerical simulation to conduct relevant research on the inundation range of the floodplain area of the lower Yellow River after the construction of flood control levees. Compared with their studies, it can be proved that the simulation results in this study are basically correct.

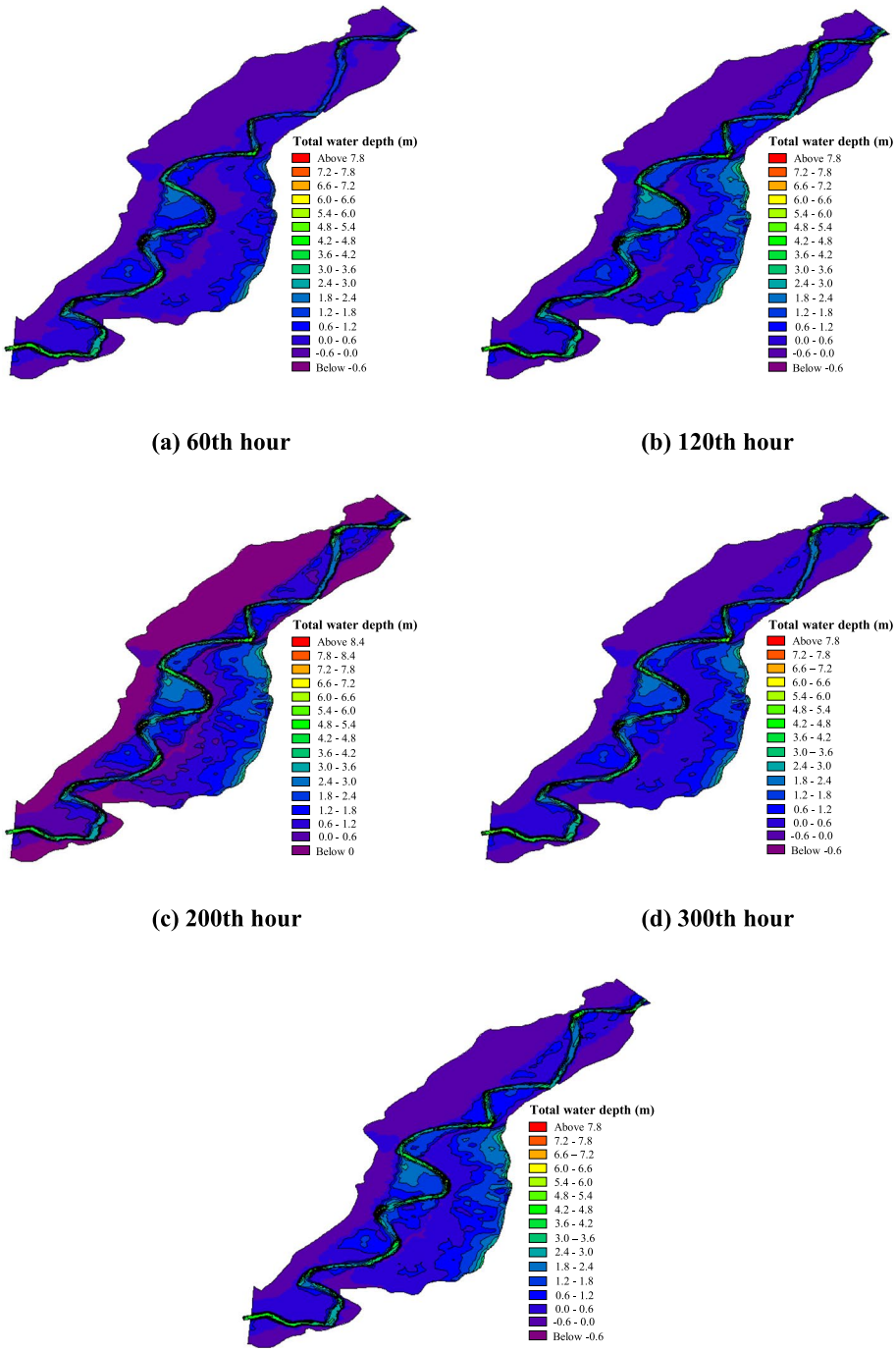

Fig. 9 Water depth and inundation range under "92.8" flood. **a** 60th h. **b** 120th h. **c** 200th h. **d** 300th h. **f** 400th h

Loss analysis

This study mainly covers the Jiahetan-Gaocun reach of the lower Yellow River, including the Dongming floodplain area and Changyuan floodplain area. The floodplain area in the lower reaches of the Yellow River has flat terrain, fertile land, and superior water

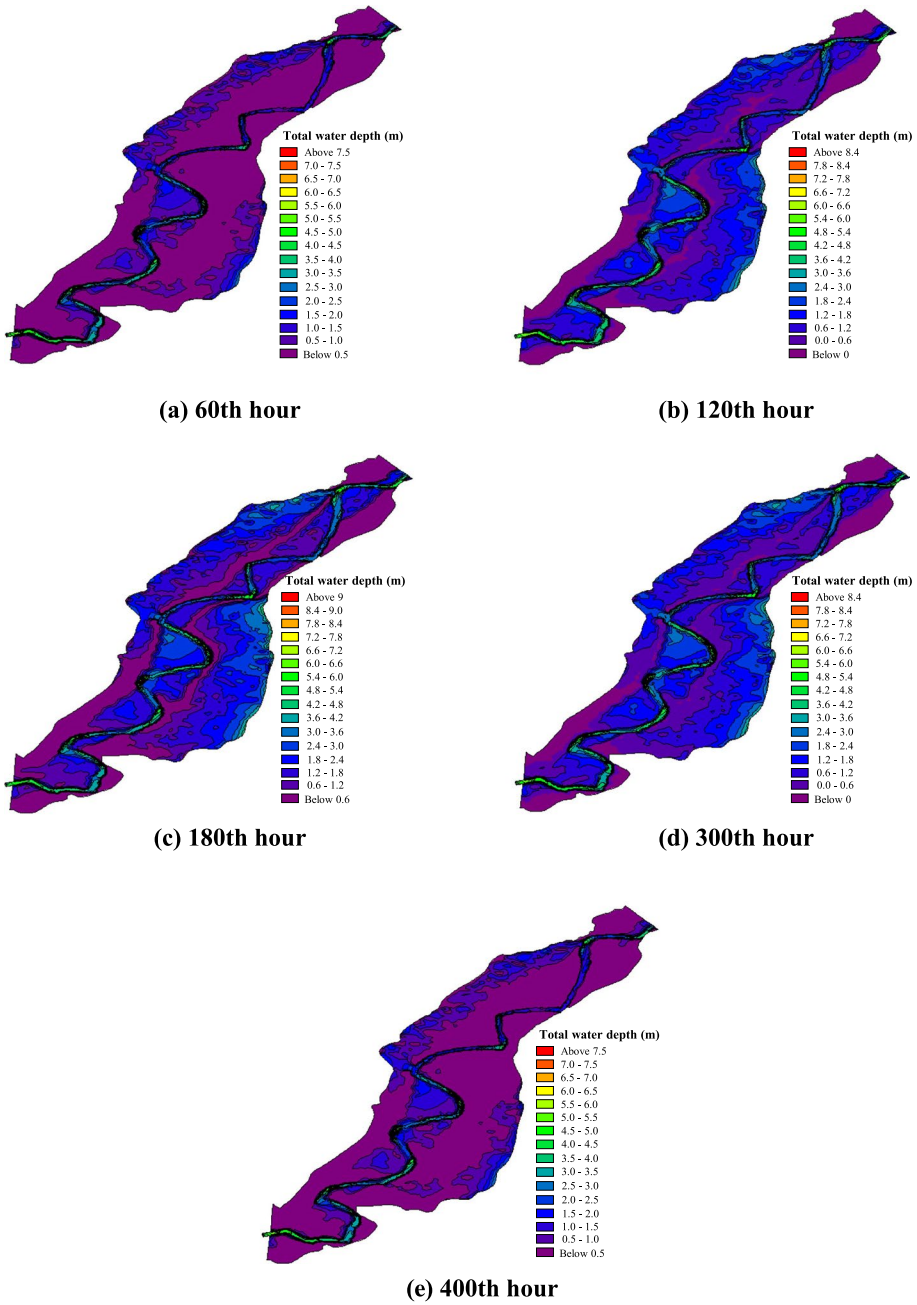

Fig. 10 Water depth and inundation range under "96.8" flood. **a** 60th h. **b** 120th h. **c** 180th h. **d** 300th h. **f** 400th h

conservancy conditions. In addition, the Yellow River flood has strong seasonality and a low probability of occurrence. Since ancient times, a large number of people have settled down. The floodplain area economy is a typical agricultural economy, and the crops are mainly wheat, soybean, corn, and cotton. Dongming floodplain area and Changyuan floodplain area in the lower reaches of the Yellow River are typically agricultural economies, and the floodplain flood in this reach mainly occurs in July and August. At this time, autumn grain is mainly planted in the floodplain area. See Table 3 for the basic socio-economic conditions of the Dongming floodplain area and Changyuan floodplain

Table 3 Economic situation of Dongming and Changyuan floodplain area

Name of the floodplain area	Area (km^2)	Cultivated land area (km^2)	Population
Dongming	234.6	134	89,670
Changyuan	322	223	112,525

area in the lower reaches of the Yellow River. In addition to the data in the table, there are brick factories, concrete prefabrication plants, tile factories, valleys, fish ponds, and lotus ponds in the Dongming floodplain area, with a total of 4,566,500 km^2, including 6 gas stations and more than 30 oil wells. There are mainly farms in the Changyuan floodplain area, with a total area of 2100 km^2.

The direct economic loss of a flood disaster refers to the loss caused by the flood impact and inundation of the disaster-bearing body. The estimation formula of the direct economic loss of a single disaster-bearing body is as follows:

$$R = \sum_{i=1}^{m} \eta_i W_i$$

where R is the direct economic loss of the disaster-bearing body, η_i is the loss rate at i level water depth, and W_i is the normal value or output value of the disaster-bearing body within the submergence range of i level water depth. It can be calculated by the following equation.

$$W_i = \frac{A_i}{A} \times V$$

where A_i is the area of this bearing body at water depth i, A is the total area of the disaster-bearing body in the area, and V is the total value or output value of the disaster-bearing body in the region.

All losses within the floodplain area are the accumulation of direct economic losses of various disaster-bearing bodies.

Liu et al. [47] investigated the loss of the Yellow River floodplain area after the 1982 flood in the analysis of flood risk and research on disaster reduction measures in the Yellow River floodplain area and flood detention area, mainly in rural areas. After research and analysis, they determined the loss rate of household property of rural residents. Concerning this study and combined with the actual situation of this study area, the water depth of different disaster-bearing body — direct economic loss rate η relationship is shown in Table 4 below.

Table 4 Water depth of different disaster-bearing bodies — direct economic loss rate η relationship

Water depth (m)	0 − 0.5	0.5 − 2.0	2 − 4.0	> 4.0
Autumn grain	70	85	100	100
Tree	0	2.5	15	20
Fisheries	50	100	100	100
House	31	71	100	100
Family property	27	50	75	85

Combined with the above table and flood routing simulation results, after analysing the inundation loss in the floodplain area, we get the following main conclusions:

1. In the early stage of flood routing, shallow water depth and medium water depth account for the majority, so the flood inundation loss rate is small. With the evolution of flood, the inundation depth increases continuously, and the inundation loss rate of various disaster-bearing bodies will also increase with the increase of inundation depth. When the inundation depth reaches a certain value, the inundation loss rate of each disaster-bearing body will reach the maximum. Zhang et al. [32] obtained a similar conclusion using the inundation loss function.
2. Compared with other disaster-bearing bodies, autumn grain and fishery are the most vulnerable to damage. Under the condition of shallow water and deep water, the loss of autumn grain and fishery has been very high. Li [48] once conducted a systematic study on the assessment of flood losses in the lower Yellow River based on GIS. The main flooded area in the lower Yellow River is cultivated land. The simulation results show that the shallow water deep area is already large in the early stage of the flood, which means that as long as the floodplain area is used as a flood storage and detention area, the loss of autumn grain and fishery is inevitable and huge. Therefore, when the floodplain area is used as flood storage and detention area, the loss of autumn grain and fishery must be considered first.

Conclusions

With global warming, the frequency of floods is increasing. Flood management strategies have recently been considered a priority, particularly in the Yellow River. Many scholars have done a lot of research on flood simulation and flood inundation loss assessment. However, in recent years, there has been little research on the lower Yellow River flood. The floodplain area in the lower Yellow River is not only an important flood storage and detention area but also inhabited by a large number of residents. Therefore, it is not easy to formulate flood management strategies when to use the floodplain of the lower Yellow River as a flood storage and detention area. In this paper, a 2D hydrodynamic model of the Jiehetan-Gaocun section in the lower Yellow River including two floodplain areas was established by the MIKE 21, followed by parameter rate determination, flood simulation calculation, and flood inundation loss assessment. The significance of this study is to explore the basic laws of flood inundation in the floodplains of the lower Yellow River and lay the foundation for formulating flood management strategies. At the same time, the research results can also provide a reference for the analysis of inundation processes in other regions of the world. The main research conclusions of this article are as follows:

1. Through the model verification of the flood, the errors of the measured flood level at each water level observation point of the calculated river section and the corresponding simulated calculated flood level are within the allowable range, which indicates that the model is reasonable in terms of the selection of the river topography and boundary treatment, roughness, and water flow parameters. The calculation

results of the flooding process and the flood separation in the lower reaches of the Yellow River using this model are credible.

2. With the validated model, the dynamic analysis of the inundation area of the floodplain area and the variation of different inundation depths with time under two working conditions were carried out in this paper, and the basic law of flood inundation in the floodplain area of Jiehetan-Gaochun River section was obtained.
3. After analysing the flood loss, we can find that autumn grain, as the most vulnerable disaster-bearing body, is the main source of income for the people in the floodplain area. The loss is huge in the early stage of flood development, so it should be considered before opening the floodplain area as a flood storage and detention area.

Acknowledgements
I would like to thank Associate Professor Jian Chen of North China University of Water Resources and Electric Power for his assistance in carrying out this research. At the same time, I thank the anonymous reviewers for constructive comments that helped improve this manuscript.

Authors' contributions
The author(s) read and approved the final manuscript.

Funding
This research did not receive any specific grant from funding agencies in the public, commercial, or not-for-profit sectors.

Availability of data and materials
The datasets used and analysed during the current study are available from the corresponding author on reasonable request.

Declarations

Competing interests
The author declares no competing interests.

Received: 23 October 2022 Accepted: 5 April 2023
Published online: 17 April 2023

References

1. Zhang S, Wu D, Li K (2021) On the theory and method of water ecological protection and restoration in the Yellow River basin. Yellow River 43(S2):93–95
2. Chen CX, Fu J, Wu MX, Gao X, Ma LM (2022) High-efficiency sediment transport requirements for operation of the Xiaolangdi Reservoir in the lower Yellow River. Water Supply 22(12):8572–8586. https://doi.org/10.2166/ws.2022.397
3. Zhao Y, Cao W, Hu C, Wang Y, Wang Z, Zhang X, Zhu B, Cheng C, Yin X, Liu B, Xie G (2019) Analysis of changes in characteristics of flood and sediment yield in typical basins of the Yellow River under extreme rainfall events. Catena 177:31–40. https://doi.org/10.1016/j.catena.2019.02.001
4. Zhou MZ, Zhou GS, Lv XM, Zhou L, Ji YH (2019) Global warming from 1.5 to 2 degrees C will lead to increase in precipitation intensity in China. Int J Climatol 39(4):2351–2361. https://doi.org/10.1002/joc.5956
5. Myhre G, Alterskjaer K, Stjern CW, Hodnebrog O, Marelle L, Samset BH, Sillmann J, Schaller N, Fischer E, Schulz M, Stohl A (2019) Frequency of extreme precipitation increases extensively with event rareness under global warming. Sci Rep 9:16063. https://doi.org/10.1038/s41598-019-52277-4
6. Tellman B, Sullivan JA, Kuhn C, Kettner AJ, Doyle CS, Brakenridge GR, Erickson TA, Slayback DA (2021) Satellite imaging reveals increased proportion of population exposed to floods. Nature 596(7870):80–86. https://doi.org/10.1038/s41586-021-03695-w
7. Qu B, Lv AF, Jia SF, Zhu WB (2016) Daily precipitation changes over large river basins in China, 1960–2013. Water 8(5). https://doi.org/10.3390/w8050185
8. Wang W, Yin S, Gao G, Papalexiou SM, Wang Z (2022) Increasing trends in rainfall erosivity in the Yellow River basin from 1971 to 2020. J Hydrol 610:127851. https://doi.org/10.1016/j.jhydrol.2022.127851
9. Ma X, Xia Q Research on resilience strategy of Yellow River floodplain area based on ecological redundancy improvement: a case study of Yellow River floodplain area in Xinxiang City. 2020/2021 China Urban Planning Annual Conference and 2021 China Urban Planning Academic Quarter, Chengdu, ate 2021. pp 280–290. https://doi.org/10.26914/c.cnkihy.2021.029749
10. Yu K, Gong Y (2021) Exploration on ecological restoration model for the improvement of ecosystem services of Yellow River floodplains — a case study of Zhengzhou Yellow River floodplain park planning and design. Landscape Architect Front 9(03):86–97

11. Liu Y, Jiang E, Wan Q, Zhang Q, Zhang Y (2016) Different governance patterns of the Yellow River beach area in flood control and disaster under current boundary. Yellow River 38(03):30–32+63. https://doi.org/10.3969/j.issn.1000-1379.2016.03.009
12. Run Y, Cui Y, Qin Y, Hu Y, Fu Y, Liu X, Shi Z, Li Q, Fan L (2021) Spatial-temporal dynamic of water and land in the Yellow River beach area based on Google Earth Engine. Yellow River 43(09):85–89+93. https://doi.org/10.3969/j.issn.1000-1379.2021.09.016
13. Su L, Lu X, Gong X (2021) Yellow River downstream flood compatibility and beach area government pattern research. Water Resour Hydropower Eng 52(S2):366–370. https://doi.org/10.13928/j.cnki.wrahe.2021.S2.079
14. Zhang J, Shang Y, Cui M, Luo Q, Zhang R (2022) Successful and sustainable governance of the lower Yellow River, China: a floodplain utilization approach for balancing ecological conservation and development. Environ Dev Sustain 24(3):3014–3038. https://doi.org/10.1007/s10668-021-01593-9
15. Zhang K, Shen J (2019) Research on China's drainage rights trading management under the quasi market: based on the perspective of evolutionary game. J Henan Univ (Social Science) 59(04):21–29
16. Zhang KZ, Dong ZC, Guo L, Boyer EW, Mello CR, Shen JQ, Lan P, Wang JL, Fan BH (2022) Allocation of flood drainage rights in the middle and lower reaches of the Yellow River based on deep learning and flood resilience. J Hydrol 615:128560. https://doi.org/10.1016/j.jhydrol.2022.128560
17. Fan Y (2005) Research and application on flood wave advance numeric modeling of one-dimension and two-dimension of rivers and flood detention area. Master's Thesis, Tianjin University, Tianjin
18. Liu P, Guo S, Xiao Y, Li W, Xiong L (2007) Study on the optimal reservoir seasonal flood control water level. J Hydro-electric Eng 26(3):5–10. https://doi.org/10.3969/j.issn.1003-1243.2007.03.002
19. Jiang S, Huang Z, Huang J, Zhang Y, Jiang X (2020) Flood evolution simulation in flood storage and detention area and evaluation methods for the dike-break losses. J Water Resour Water Eng 31(01):131–139145. https://doi.org/10.11705/j.issn.1672-643X.2020.01.20
20. Bhowmik NG Impacts of the 1993 flood on the Mississippi River in Illinois. Hydraulic Engineering, Reston, ate 1994. ASCE, pp 613–617
21. Jonkman SN (2007) Loss of life estimation in flood risk assessment: theory and applications. Doctoral Thesis, Delft University, Netherlands
22. Chinh DT, Gain AK, Dung NV, Haase D, Kreibich H (2016) Multi-variate analyses of flood loss in Can Tho City. Mekong Delta Water 8(1):6
23. Zhao L, Zhang T, Fu J, Li J, Cao Z, Feng P (2021) Risk assessment of urban floods based on a SWMM-MIKE21-coupled model using GF-2 data. Remote Sens 13(21):4381
24. Guo P, Xia J, Chen Q, Li N (2017) A mechanics-based model of flood risk assessment and its application in a flood diversion zone. Adv Water Sci 28(06):858–867. https://doi.org/10.14042/j.cnki.32.1309.2017.06.007
25. Gemmer M, Wang G, Tong J (2006) Dynamic inundation risk identification and estimation of the potential loss in Honghu flood diversion area, China. J Lake Sci 18:464–469. https://doi.org/10.18307/2006.0504
26. Ruidas D, Chakrabortty R, Islam ARMT, Saha A, Pal SC (2022) A novel hybrid of meta-optimization approach for flash flood-susceptibility assessment in a monsoon-dominated watershed, eastern India. Environ Earth Sci 81(5):145. https://doi.org/10.1007/s12665-022-10269-0
27. Ruidas D, Saha A, Islam ARMT, Costache R, Pal SC (2022) Development of geo-environmental factors controlled flash flood hazard map for emergency relief operation in complex hydro-geomorphic environment of tropical river, India. Environ Sci Pollut Res. https://doi.org/10.1007/s11356-022-23441-7
28. Roy P, Chandra Pal S, Chakrabortty R, Chowdhuri I, Malik S, Das B (2020) Threats of climate and land use change on future flood susceptibility. J Cleaner Prod 272:122757. https://doi.org/10.1016/j.jclepro.2020.122757
29. Schröter K, Lüdtke S, Redweik R, Meier J, Bochow M, Ross L, Nagel C, Kreibich H (2018) Flood loss estimation using 3D city models and remote sensing data. Environ Model Softw 105:118–131. https://doi.org/10.1016/j.envsoft.2018.03.032
30. Wang Y, Li N, Wang S, Wang J, Zhang N (2019) Development and application of flood damage assessment system. J Hydraulic Eng 50(09):1103–1110. https://doi.org/10.13243/j.cnki.slxb.20190350
31. James L, Lee R (1971) Economics of water resources planning. McGraw-Hill Inc., New York
32. Zhang X, Zhang H, Li Y, Sun D (2015) Research on floodplain flood loss assessment of the lower Yellow River. Syst Eng-Theory Pract 35(6):1625–1632. https://doi.org/10.12011/1000-6788(2015)6-1625
33. Jia P, Wang Q, Lu X, Zhang B, Li C, Li S, Li S, Wang Y (2018) Simulation of the effect of an oil refining project on the water environment using the MIKE 21 model. Phys Chem Earth Parts A/B/C 103:91–100. https://doi.org/10.1016/j.pce.2017.02.003
34. Liu X, Liu G, Wang Z (2020) The study and application of flood simulation at detention basin based on MIKE series model. China Rural Water Hydropower 6:10-15,20. https://doi.org/10.3969/j.issn.1007-2284.2020.06.002
35. Chen P, Fu C, Yu J, Ji X (2017) Research on the numerical simulation of flood routing for the flood detention basin based on MIKE 21. China Rural Water Hydropower 8:113-116,120. https://doi.org/10.3969/j.issn.1007-2284.2017.08.024
36. Zhang XL, Li XJ (2012) 2-D flood routing simulation on the lower Yellow River from Huayuankou to Jianetan based on MIKE21 software. Appl Mech Mater 170–173:1021–1024
37. Ruidas D, Pal SC, Saha A, Chowdhuri I, Shit M (2022) Hydrogeochemical characterization based water resources vulnerability assessment in India's first Ramsar site of Chilka Lake. Marine Pollut Bull 184:114107. https://doi.org/10.1016/j.marpolbul.2022.114107
38. Ruidas D, Pal SC, Islam ARMT, Saha A (2021) Characterization of groundwater potential zones in water-scarce hardrock regions using data driven model. Environ Earth Sci 80(24):809. https://doi.org/10.1007/s12665-021-10116-8
39. Ruidas D, Pal SC, Towfiqul Islam ARM, Saha A (2023) Hydrogeochemical evaluation of groundwater aquifers and associated health hazard risk mapping using ensemble data driven model in a water scares plateau region of eastern India. Exposure Health 15(1):113–131. https://doi.org/10.1007/s12403-022-00480-6

40. Pal SC, Ruidas D, Saha A, Islam ARMT, Chowdhuri I (2022) Application of novel data-mining technique based nitrate concentration susceptibility prediction approach for coastal aquifers in India. J Clean Prod 346:131205. https://doi.org/10.1016/j.jclepro.2022.131205
41. Zhang X, Duan B, He S, Lu Y (2022) Simulation study on the impact of ecological water replenishment on reservoir water environment based on MIKE21——taking Baiguishan Reservoir as an example. Ecol Indicators 138:108802. https://doi.org/10.1016/j.ecolind.2022.108802
42. Zhang X, Zhao D, He S (2022) Simulation study on the influence of bridge pier spacing on the flow pattern of the lower Yellow River. Iranian J Sci Technol Transact Civil Eng 46(6):4665–4675. https://doi.org/10.1007/s40996-022-00901-1
43. Zhao DH, Shen HW, Tabios GQ, Lai JS, Tan WY (1994) Finite-volume two-dimensional unsteady-flow model for river basins. J Hydraul Eng 120(7):863–883. https://doi.org/10.1061/(ASCE)0733-9429(1994)120:7(863)
44. Sleigh PA, Gaskell PH, Berzins M, Wright NG (1998) An unstructured finite-volume algorithm for predicting flow in rivers and estuaries. Comput Fluids 27(4):479–508. https://doi.org/10.1016/S0045-7930(97)00071-6
45. Chen J, Jian L, Zou Z, Hou Y (2014) Study of flood-control function of flood diversion and dentension by utilizing floodplain in lower Yellow River. Eng J Wuhan Univ 47(01):8–11
46. Wang M, Dong H, Bi G, Zhang F (2019) Impact of protection embankment construction on typical floods and flood control. Yellow River 41(02):35–38
47. Liu S, Song Y, Cheng X, Liu H, Huang J, Li Y, Chen H, Zhang Y (1999) Risk analysis and disaster reduction countermeasures of the Yellow River floodplain area and flood storage and detention area. Yellow River Water Conservancy Press, Zhengzhou
48. Li L (2019) Study on flood loss assessment and disaster reduction strategies in the middle and lower reaches of the Yellow River in Henan province. Master's Thesis, Henan Polytechnic University

Publisher's Note